# South Atlantic Variability Arising from Air–Sea Coupling: Local Mechanisms and Tropical–Subtropical Interactions

SYLWIA TRZASKA AND ANDREW W. ROBERTSON

*International Research Institute for Climate and Society, The Earth Institute at Columbia University, Palisades, New York*

JOHN D. FARRARA* AND CARLOS R. MECHOSO

*Department of Atmospheric Sciences, University of California, Los Angeles, Los Angeles, California*

(Manuscript received 23 January 2006, in final form 22 August 2006)

ABSTRACT

Interannual variability in the southern and equatorial Atlantic is investigated using an atmospheric general circulation model (AGCM) coupled to a slab ocean model (SOM) in the Atlantic in order to isolate features of air–sea interactions particular to this basin. Simulated covariability between sea surface temperatures (SSTs) and atmosphere is very similar to the observed non-ENSO-related covariations in both spatial structures and time scales. The leading simulated empirical coupled mode resembles the zonal mode in the tropical Atlantic, despite the lack of ocean dynamics, and is associated with baroclinic atmospheric anomalies in the Tropics and a Rossby wave train extending to the extratropics, suggesting an atmospheric response to tropical SST forcing. The second non-ENSO mode is the subtropical dipole in the SST with a mainly equivalent barotropic atmospheric anomaly centered on the subtropical high and associated with a midlatitude wave train, consistent with atmospheric forcing of the subtropical SST.

The power spectrum of the tropical mode in both simulation and observation is red with two major interannual peaks near 5 and 2 yr. The quasi-biennial component exhibits a progression between the subtropics and the Tropics. It is phase locked to the seasonal cycle and owes its existence to the imbalances between SST–evaporation and SST–shortwave radiation feedbacks. These feedbacks are found to be reversed between the western and eastern South Atlantic, associated with the dominant role of deep convection in the west and that of shallow clouds in the east. A correct representation of tropical–extratropical interactions and of deep and shallow clouds may thus be crucial to the simulation of realistic interannual variability in the southern and tropical Atlantic.

## 1. Introduction

Successful seasonal prediction for regions surrounding the tropical Atlantic remains particularly challenging with skills hampered by the inability of the current systems to correctly predict SST in the tropical Atlantic (Goddard and Mason 2002). The basin supports a range of modes of variability and is strongly dominated by longer, decadal time scales (Mehta and Delworth 1995; Tourre et al. 1999) and external influences, and part of the predictability arises from interannual persistence and delayed ENSO influence (Mehta and Delworth 1995; Mo and Häkkinen 2001; Saravannan and Chang 2004) while the actual SST anomalies may also interfere with the ENSO signal in the region (Giannini et al. 2004; Huang et al. 2005).

The dominant modes of variability in the tropical Atlantic are the so-called meridional (or transequatorial) and zonal (or equatorial) modes, the former being rather boreal winter-to-spring mode with clear decadal component (Enfield and Mayer 1997; Chang et al. 2000; Ruiz-Barradas et al. 2000), the latter rather boreal summer-to-fall and interannual (Houghton and Tourre 1992; Zebiak 1993; Carton and Huang 1994; Ruiz-Barradas et al. 2000; Mo and Häkkinen 2001). Authors

* Current affiliation: Raytheon Intelligence and Information Systems, Pasadena, California.

*Corresponding author address:* Sylwia Trzaska, International Research Institute for Climate and Society, 202 Monell Building, P.O. Box 1000, Palisades, NY 10964-8000.
E-mail: syl@iri.columbia.edu

DOI: 10.1175/JCLI4114.1

disagree as to whether these modes are fully self-sustained or triggered by external forcings such as ENSO (Zebiak 1993; Carton and Huang 1994; Delecluse et al. 1994; Chang et al. 1997, 2000; Ruiz-Barradas et al. 2000; Mo and Häkkinen 2001; Saravannan and Chang 2004) and how they relate to each other (Servain and Dessier 1999; Murtugudde et al. 2001). Some evidence has also been found for relationships between tropical and extratropical latitudes, especially in the northern Atlantic (Robertson et al. 2000; Okumura et al. 2001).

However, the equatorial Atlantic and the cold tongue complex are more open to the South Atlantic and isolated from the northern basin, indicating potential for interactions with southern subtropical Atlantic via the southeast trade system. Indeed, Robertson et al. (2003) found an evolution from the subtropical to more tropical anomalies in the South Atlantic from January–March to April–June seasons, and Barreiro et al. (2004) isolated preconditions during boreal summer leading to the onset of the transequatorial gradient in subsequent boreal spring, captured by an atmospheric GCM coupled to a mixed-layer oceanic model. Similarly, Carton and Huang (1994) and Florenchie et al. (2004) found evidence of connections between equatorial and southeastern Atlantic via ocean dynamics. Yet, the connections between the tropical and extratropical regions in South Atlantic have not been extensively documented: when including a substantial portion of extratropics in the study domain, as in Venegas et al. (1996), Sterl and Hazeleger (2003), or Robertson et al. (2003), the analyses tend to focus on the so called subtropical dipole arising as dominant coupled pattern due to higher amplitude of variability in subtropical/extratropical regions as opposed to the tropical ones; conversely most of the studies mentioned earlier focusing on the tropical variability only extend to 20°S, excluding analyses of tropical–extratropical interactions.

In this paper we examine interannual variability associated with thermodynamic interactions between the atmosphere and the upper-ocean mixed layer over the South and tropical Atlantic, using an atmospheric general circulation model (AGCM) coupled to a slab ocean model (SOM) in the Atlantic region. By prescribing climatological SSTs outside of the Atlantic basin, we isolate variability that is intrinsic to the Atlantic. The model and observed datasets are described in section 2, and the main characteristics of the variability simulated by the model in South Atlantic are presented in section 3, while section 4 focuses on one particular aspect of this variability in the quasi-biennial range. A brief summary and discussion follow in section 5.

## 2. Model and data

The atmospheric component is the version 7.1 of the University of California, Los Angeles (UCLA) AGCM run with the 2.5° by 2° horizontal resolution and 29 layers in vertical. The AGCM has been coupled to a constant 50-m-deep slab ocean model (SOM) over the Atlantic basin (50°S–50°N) allowing the SST to respond to and feed back on the atmospheric heat fluxes solely in this region while climatological SST values were prescribed elsewhere. The heat transport by the ocean, absent by construction from the SOM, is parameterized by climatological "Q flux" derived from a 20-yr control run of the same AGCM forced by climatological SST. An additional relaxation term to climatology with a 60-day time scale was also necessary. The UCLA-SOM was run for 34 yr, of which we analyze the last 29 yr.

Several major revisions have recently been made to the UCLA AGCM. The formulation of moist processes in the PBL and moisture exchange with the layer above has been revised (Li et al. 2002), resulting in a greatly improved geographical distribution of PBL stratus cloud. A new parameterization of gravity wave drag due to subgrid-scale orography has been implemented. The effects of convective downdrafts and vertical momentum and rainwater budgets are being included in the cumulus parameterization. Cumulus convection, including its interaction with the PBL, follows the prognostic Arakawa–Schubert scheme of Pan and Randall (1998). Cloud liquid water and ice are explicitly predicted (Köhler 1999). Full details can be found online at http://www.atmos.ucla.edu/~mechoso/esm/agcm.html. Improvements achieved so far have resulted in a superior simulation of the mean climate and interannual variability in the tropical Pacific, including the warm pool, equatorial cold tongue and its dominant semi−annual cycle, and ENSO intensity, evolution, and structure (Yu and Mechoso 2001; Li et al. 2002).

Some of the results are compared to the data from the National Centers for Environmental Prediction–National Center for Atmospheric Research (NCEP–NCAR) reanalysis (Kalnay et al. 1996) over the period 1949–2002, used as surrogate to observations. In a recent analysis of air–sea interactions in the tropical Atlantic Frankignoul and Kestenare (2005) used the NCEP–NCAR reanalysis data after Frankignoul and Kestenare (2002) had compared the air–sea fluxes from the reanalysis to the observed ones from the Comprehensive Ocean–Atmosphere Data Set (COADS) and found only a slight negative bias. Here however the reanalyzed data are not used to infer mechanisms, only to document the main patterns of variability, strongly

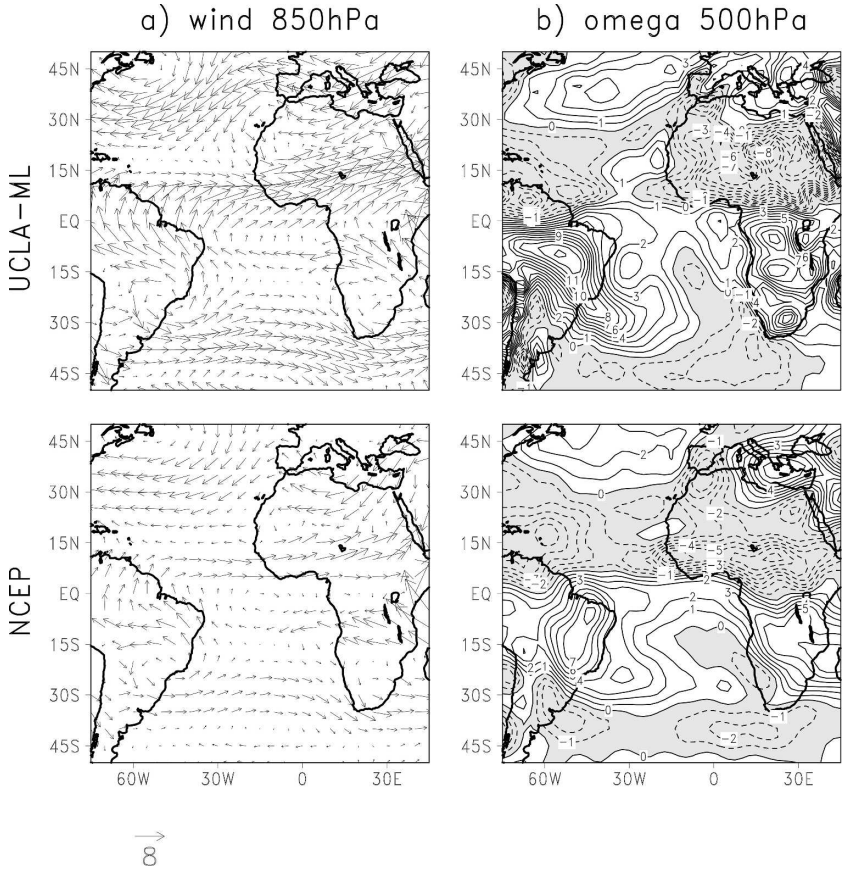


FIG. 1. Seasonal cycle as difference between July–September and January–March means simulated by (top) UCLA-SOM and (bottom) NCEP reanalysis: (a) seasonal changes in wind at 850 hPa (in m $s^{-1}$; scale in lower-left area); (b) seasonal changes in vertical velocity at 500 hPa (in $10^{-2}$ Pa $s^{-1}$; negative values, shaded, for enhanced upward motion).

constrained by observed SST, to assess the realism of model's variability.

Figure 1 illustrates model performance in the Atlantic region in simulating the average seasonal (upper panels) as compared to the NCEP reanalysis fields (lower panels) expressed as the difference between seasonal July-to-September minus January-to-March means of low-level circulation and midtropospheric vertical velocity. The simulated seasonal cycle is realistic, although the amplitude of the low-level wind seasonal changes is overestimated. In particular, the model generates a well-defined South American summer monsoon, South Atlantic convergence zone (SACZ) in austral summer and West African monsoon during boreal summer. The simulated variability of the surface temperature is evaluated in Fig. 2 in terms of variance of the monthly departures from the mean seasonal cycle. The amplitude of variability agrees well over the land where the temperature is produced by models' surface schemes with little influence from the observations in the reanalysis. Over the ocean, where the reanalysis data are based on observations—the Met Office (UKMO) Global Sea Ice and SST dataset (GISST; Rayner et al. 1996), for the pre-1982 period and optimum interpolation (OI) SST (Reynolds and Smith 1994) afterward—UCLA-SOM greatly overestimates the variability in the southeastern Atlantic, in the region of the stratus deck (cf., e.g., Philander et al. 1996), pointing to an overestimated sensitivity of the model stratus but also to the role of processes absent from the model such as dynamical changes in the local upwelling and emergence of the subsurface anomalies (Florenchie et al. 2004).

## 3. Empirical modes of ocean–atmosphere covariability in the South Atlantic

### *a. Singular value decomposition*

As a first step to describe the main characteristics of the coupled ocean–atmosphere variability in the South

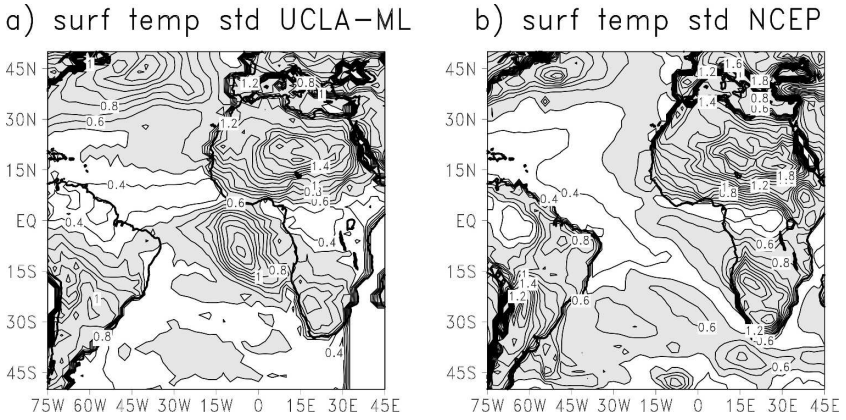


FIG. 2. Standard deviation of surface temperature (isolines every 0.1 K) for (a) UCLA-SOM 29-yr simulation and (b) NCEP 1949–2002.

Atlantic a singular value decomposition (SVD; Bretherton et al. 1992) is computed from the correlation matrix between fields of monthly surface temperature (ST) and sea level pressure (SLP) over the region within 50°S–10°N, 75°W–45°E. The results are not very sensitive to a few degree shifts in the spatial window, as long as the domain does not extend appreciably into the Northern Hemisphere. For the NCEP reanalysis, because of the presence of a strong very low frequency component in the raw data, time series for each grid point have been linearly detrended prior to the SVD analysis.

The choice of the correlation matrix, where the time series of each variable at each grid point is normalized by its standard deviation, tends to emphasize tropical anomalies relative to extratropical ones when compared to the analysis of cross-covariance used by Venegas et al. (1996, 1997) and Sterl and Hazeleger (2003). The covariability between the two normalized fields accounts for similar amounts of the combined correlation in both cases, respectively 28.2% for UCLA-SOM and 21.6% for NCEP, and the three leading modes represent respectively 84% and 70% of the squared correlation, similar to the part of variance of the three leading modes of Venegas et al. (1996).

Figures 3 and 4 show the three leading SVD modes in terms of homogeneous correlation maps for the UCLA-SOM and NCEP reanalysis respectively (in the latter case global projections are shown to identify any remote associations). The leading mode accounts for 64% of the squared correlation fraction in the UCLA-SOM ST and SLP fields over Atlantic while it represents only 34% in the reanalysis data, emphasizing the contribution of other types of variability to the total variance in the region. The ST correlation field is very similar in both cases, and is dominated by large positive correlations over the tropical South Atlantic, with a region of weaker negative correlations over the southwestern South Atlantic. This ST field is associated with basin-scale negative SLP correlations, centered over the eastern equatorial Atlantic. In both cases the negative SLP correlations extend over Africa and as far as southeastern Asia (not shown for the GCM), a pattern indicative of a response of the tropical atmosphere to SST anomalies and consistent with tropical wave dynamics (Gill 1980). In the GCM there is an additional association with SLP overlaying the reversed ST anomalies in the southwestern South Atlantic, a feature pointing to a forcing of the extratropical atmosphere from the Tropics and investigated below.

The third SVD mode (7.5% and 17.7% and of the squared correlation in model and reanalysis respectively) is also very similar between the UCLA-SOM and the reanalysis. It consists of diagonally NW–SE-oriented positive ST anomalies across the South Atlantic, accompanied by north–south dipolar SLP anomalies, with negative anomalies in the subtropics of the South Atlantic (further southward in the reanalysis). The ST–SLP correlation structure is similar to the *leading* mode found in Venegas et al. (1996) and Sterl and Hazeleger (2003), where an SVD of the *covariance* matrix was used.

The second SVD mode of the reanalysis (18.4% squared correlation) is associated with ENSO, with no counterpart in the model. The model's second SVD mode (13.2% squared correlation) is largely associated with temperature and pressure variations over South America extending into the ocean in the region of the SACZ.

Figure 5 further shows correlation patterns of different atmospheric fields with the SST SVD1 and SVD3

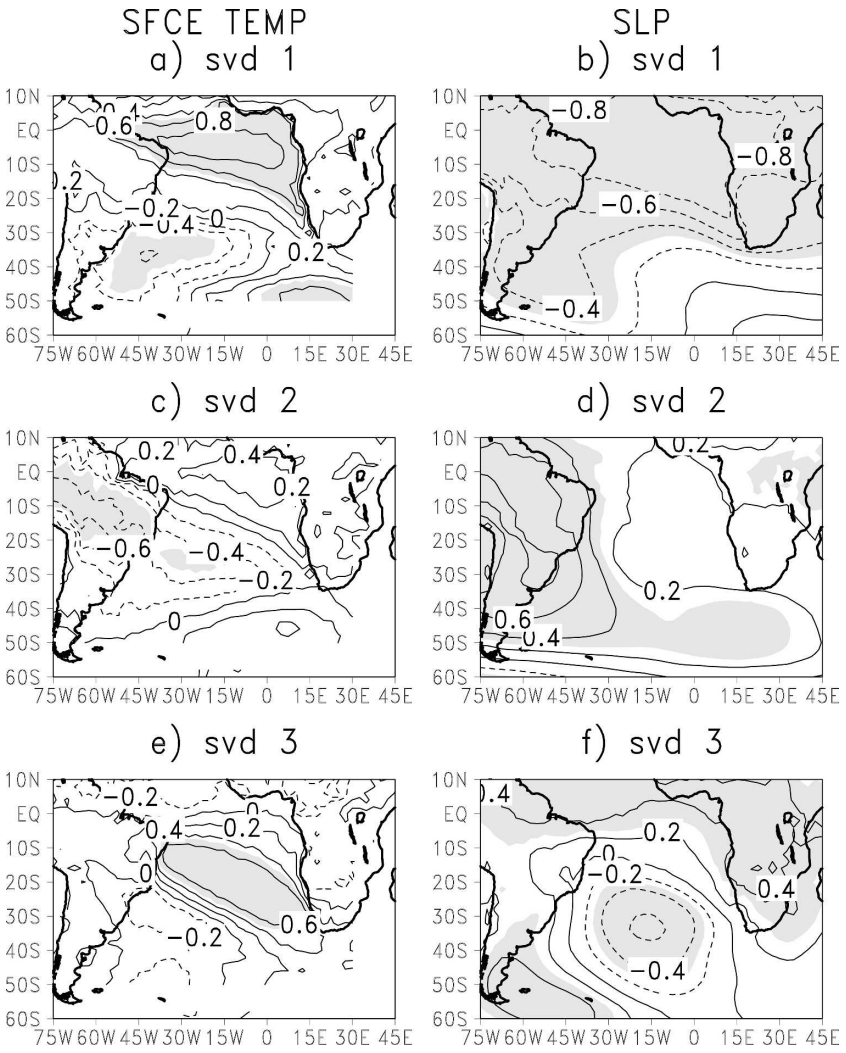


FIG. 3. Maps of homogeneous correlation coefficients between the three leading SVD principal components (PCs) and time series of individual grid points for NCEP 1949–2002. (left) Surface temperature; (right) mean sea level pressure. Contour every 0.2, shadings for correlations significant at $p = 0.05$, based on effective degrees of freedom of respective PC.

from model outputs. In the SVD1 case the lower- and upper-level wind anomalies (Figs. 5a and 5c) reveal a Matsuno–Gill-type baroclinic structure, the hallmark of a forced atmospheric response to an equatorial heat source. The low-level zonal wind anomalies peak just south of the equator, as is also the case in observations for the equatorial mode (e.g., Zebiak 1993). Wind anomalies converge slightly south of the SST anomaly as in Frankignoul and Kestenare (2005). The simulated pattern is consistent with the structures of the diabatic heating identified from observed data by Ruiz-Barradas et al. (2000) and very similar to that found in the UCLA AGCM when forced with an Atlantic SST anomaly that closely resembles SVD1 (Robertson et al. 2003): anomalously warm waters in the equatorial Atlantic coincide with enhanced upward motion (Fig. 5b) pointing to atmospheric response to equatorial SST as essential interaction leading to this mode. At upper levels twin anticyclones straddle the equator with a clear Rossby wave response and a wave train extending into the extratropical South Atlantic, similar to the one obtained in the SST-forced case by Robertson et al. (2003). The pressure anomaly over the southwestern South Atlantic seen in Fig. 3b is equivalent barotropic in the vertical and is clearly associated with this wave train—it can thus be interpreted as tropically forced. This, in turn, suggests that the negative SST anomalies in the southwestern Atlantic in SVD1 are a result of

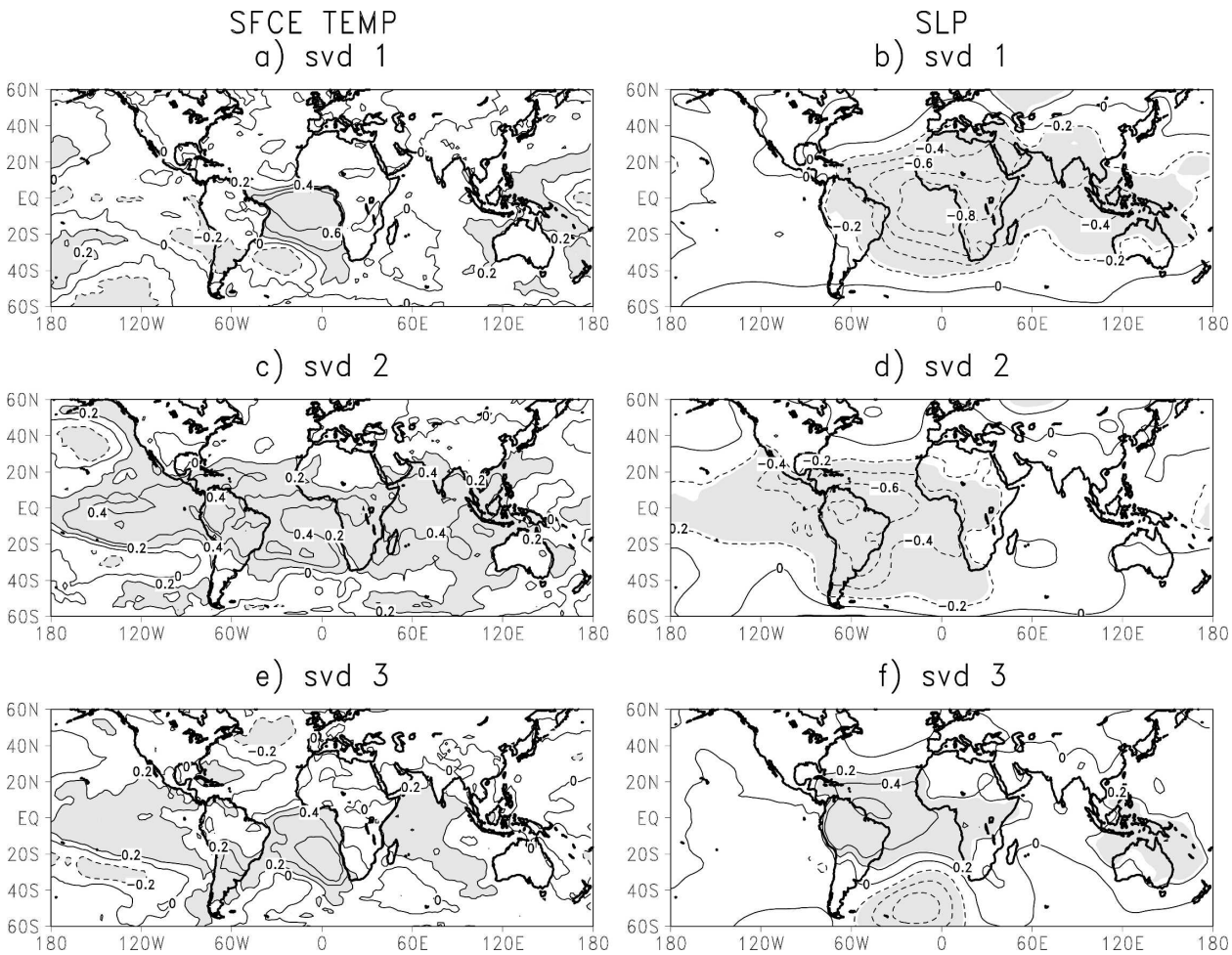


FIG. 4. Maps of homogeneous correlation coefficients between the leading SVD PCs and time series of individual grid points in the UCLA-SOM simulation. (left) Surface temperature; (right) mean sea level pressure. Contour every 0.2, shadings for correlations significant at $p = 0.05$, based on effective degrees of freedom of respective PC.

tropical forcing, through the Rossby wave train "atmospheric bridge" shown in Fig. 5c.

Despite the small fraction of squared correlation that the model's SVD3 accounts for in our analysis, its associated low-level wind anomalies (Fig. 5d) confirm the similarity of this mode with the leading mode of subtropical variability isolated by Venegas et al. (1997) and Sterl and Hazeleger (2003): warm subtropical SST anomalies are clearly associated with a reduction in the strength of the subtropical anticyclone. The geopotential height anomalies in Fig. 5e also show a clear association with a midlatitude wave train emanating from the South Pacific similar to the one generated by extratropical atmospheric adjustment to ENSO conditions (Cook 2001; Mo 2000). Since in this work no ENSO forcing is introduced in the tropical Pacific, this is indicative of the forcing of this mode by internal atmospheric variability and points to air–sea feedbacks in further strengthening and persistence of the SST structure. Note that the atmospheric anomalies have a baroclinic structure over the equatorward edge of the warm SST anomalies and equivalent barotropic atmospheric anomalies overly cooler waters of the poleward part of the SST dipole, in agreement with the results of Haarsma et al. (2003) and the forced response obtained by Robertson et al. (2003). Chaves and Nobre (2004) also found a positive feedback in the subtropical region with SACZ intensified over warm waters and a negative feedback in the southwestern Atlantic, possibly linked to the variations in the shortwave radiation.

Following previous studies that emphasized the importance of seasonality of the modes (cf. Venegas et al. 1996; Houghton and Tourre 1992; Zebiak 1993; Carton and Huang 1994; Ruiz-Barradas et al. 2000) lagged regressions of SST and SLP anomalies onto SVD1 and SVD3 (not shown) indicate that SVD3 tends to lead

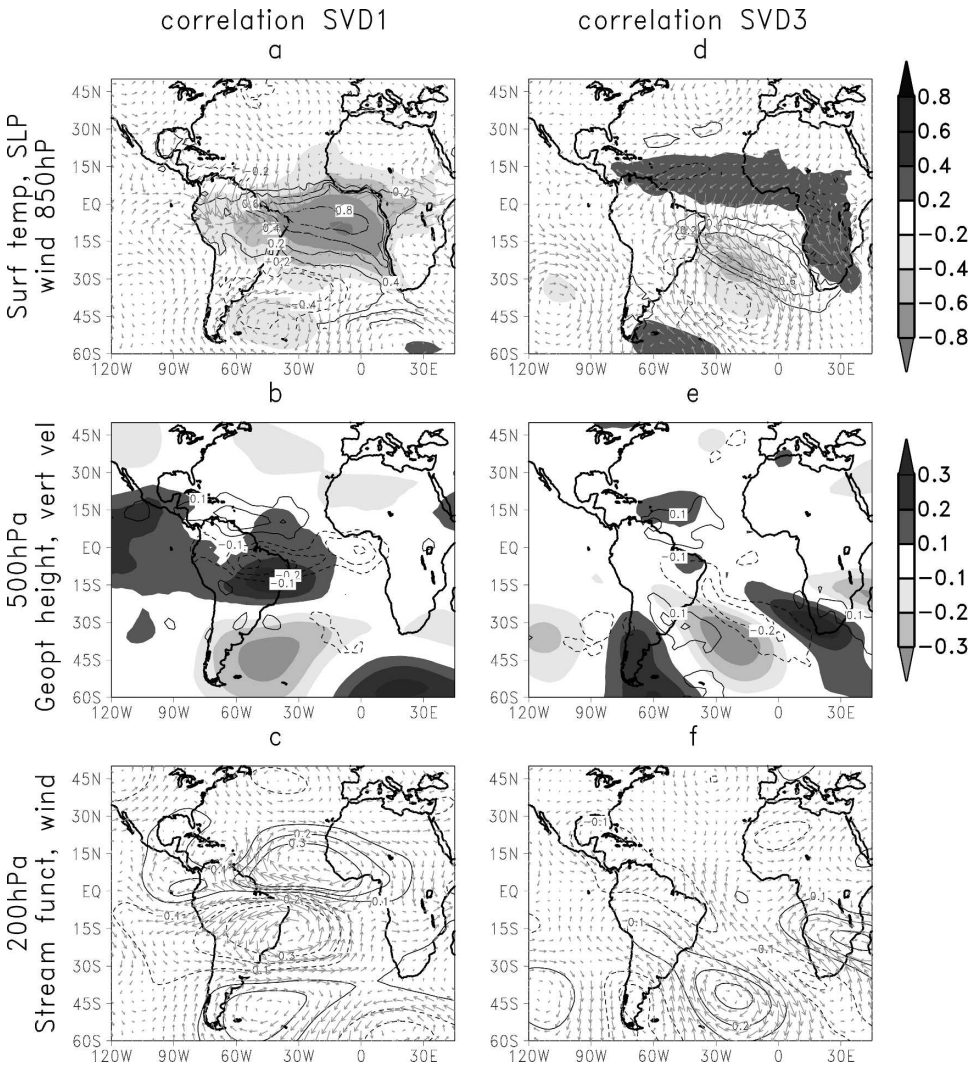


FIG. 5. Map of correlation coefficients between the leading SVD PCs of surface temperature in the UCLA-SOM simulation and (top) surface temperature (contours, every 0.2, zero line omitted), SLP (shadings, every 0.2, cf. color scale), and wind at 850 hPa; (middle) 500-hPa vertical velocity (contours, every 0.1, zero line omitted) and geopotential height (shading, cf. color scale); and (bottom) 200-hPa streamfunction (contours, every 0.1, zero line omitted) and wind.

SVD1 in both the model and the NCEP reanalysis in agreement with the seasonal progression seen in seasonal EOFs of SST over the South Atlantic (Robertson et al. 2003).

### *b. Spectral characteristic*

To further investigate the similarity between simulated and observed variability, temporal characteristics are analyzed, focusing on the leading, tropical mode, since there is some indication of possible evolution from the subtropical to tropical mode. The leading mode is also less subject to orthogonality constraints and may reflect more physical phenomena.

The power spectra of the SVD1 ST time series are plotted in Fig. 6, for both the model and reanalysis. Two contrasting spectral methods were used to check the robustness of the results: the multitaper method (MTM), and singular spectrum analysis (SSA). The spectra were computed from the monthly time series, and the plots truncated at 0.1 cycles month$^{-1}$ to emphasize the lower frequencies. Statistical significance is estimated against a first-order autoregressive process null hypothesis, using the tests of Allen and Smith (1996) for SSA and Mann and Lees (1996) for MTM; all computations were done using the UCLA SSA–MTM toolkit (Ghil et al. 2002). Both spectra are red, with a

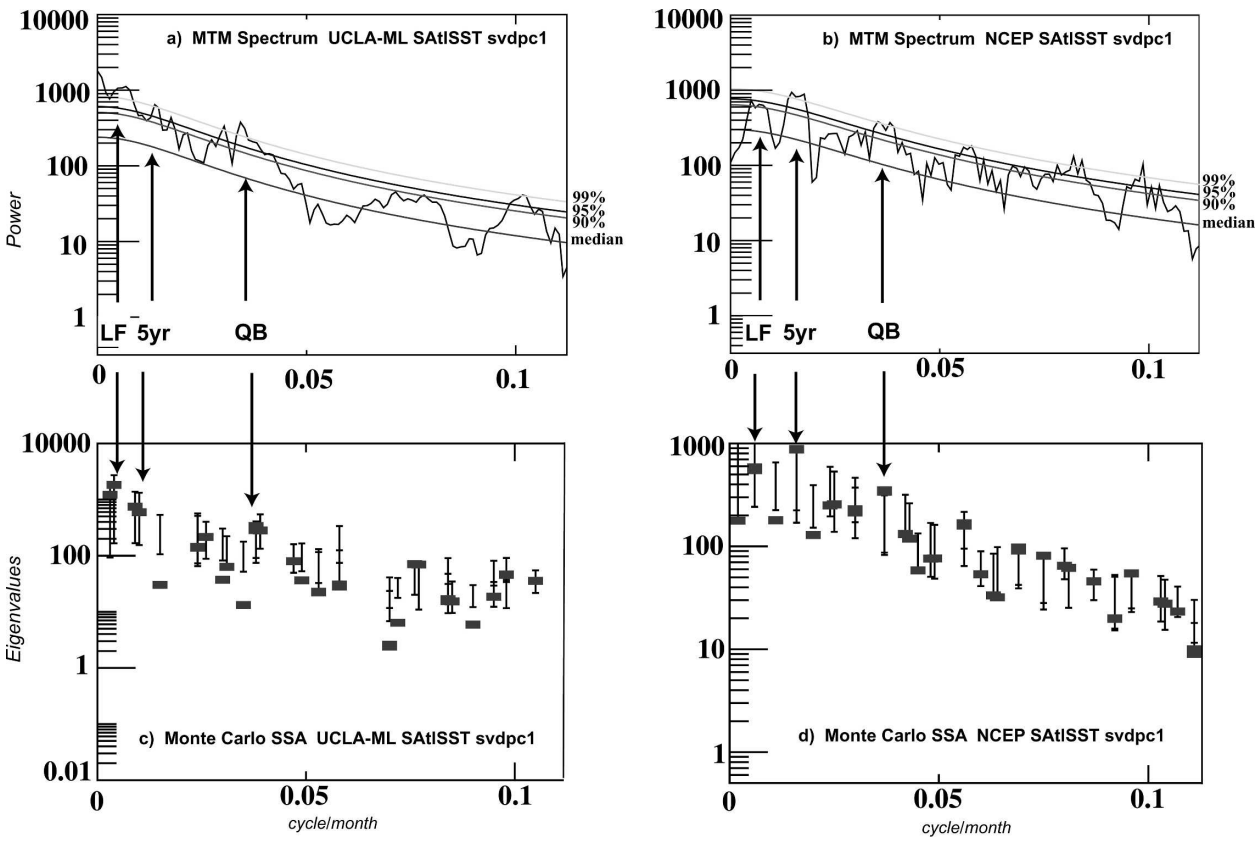


FIG. 6. (a), (b) MTM Power spectrum and (c), (d) Monte Carlo SSA decompositions of the surface temperature PCs of the leading SVD modes for (a), (c) the UCLA-SOM experiment and (b), (d) NCEP 1949–2002 (only part of the spectrum is shown). For MTM analysis the resolution has been set to 2 and the number of tapers to 3, which is thought to be the best compromise for climate signals (Mann and Park 1993). For SSA analysis a wide range of window lengths were tested and the results for a window length M = 168 months are shown; windows shorter than 100 months did not clearly separate the QB and 5-yr scales, although Vautard et al. (1992) suggest that SSA is typically successful in analyzing periods in the range [M/5, M].

very strong low-frequency component at the lowest resolved frequencies in the model's spectrum while this component is moderate in the reanalysis SVD1 due to prior detrending of the data. In the interannual range, both MTM spectra (upper panels) exhibit similar significant peaks in the ranges 26–29 and 55–60 months (labeled respectively QB and 5 yr hereafter), which coincide with the leading eigenmode pairs in the SSA analysis (lower panels), indicative of oscillatory components. These SSA pairs are statistically significant at close to the 90% level in the NCEP time series, and less statistically significant in the shorter model time series. The correspondence between 99%-significant MTM peaks and leading SSA eigenmode pairs lends credence to the assertion that the UCLA-SOM's leading mode of variability shares dominant time scales with observations.

Reconstructions of the SVD1 ST time series using the leading three SSA pairs are plotted in Fig. 7, accounting for ca. 80% of the variance of model's time series, and 50% for the reanalysis. The low-frequency pair reflects decadal persistence of same-sign anomalies for example during years 10–20 of the simulation, and 1975–84 in the reanalysis. The 5-yr component captures well-defined multiyear events, while the QB component represents fluctuations within these events. The associated spatial patterns (not shown), both exhibit NE/SW SST dipolar structures similar to the original SVD pattern and each accounts for up to 20% of the unfiltered variance in the south equatorial Atlantic in the model outputs, but the 5-yr scale is associated with variability within the deep Tropics and has some trans-equatorial links while the QB mode is more confined in the tropical and subtropical South Atlantic.

Several studies have isolated similar time scales in the equatorial and South Atlantic: the QB and ca. 4–5-yr variability have been documented in the South Atlantic by Mehta and Delworth (1995), in rainfall in Bra-

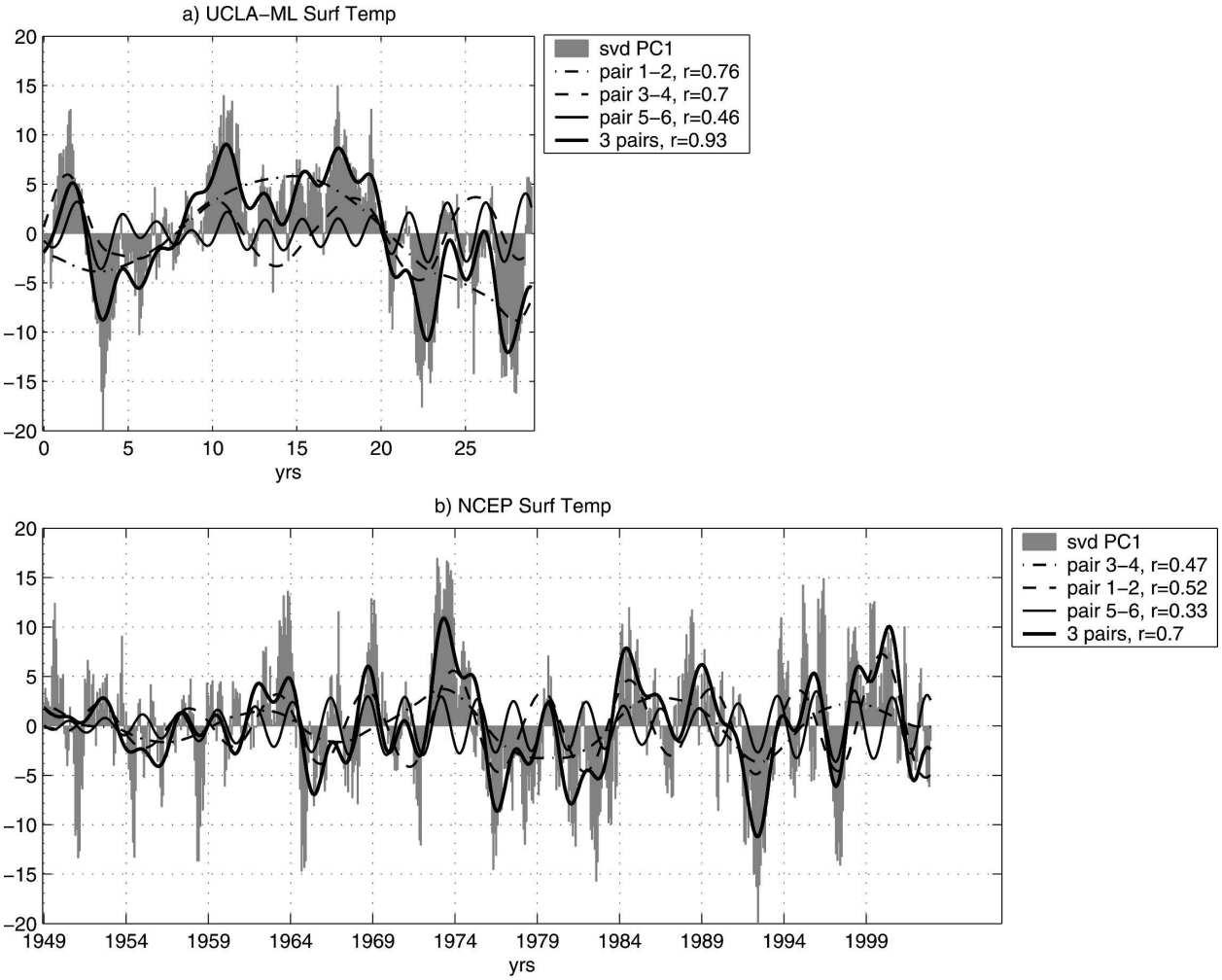


FIG. 7. Leading SVD PC for surface temperature (bars), reconstructed components (RPCs) of leading SSA pairs (dot–dash, dashed, and solid lines), and time series reconstruction based on the three RPCs for (a) UCLA-SOM and (b) NCEP.

zil by Mehta (1998), in tropical Atlantic SST by Tourre et al. (1999), and associated with ENSO forcings via extratropical Pacific South American (PSA) patterns by Mo (2000). Ruiz-Barradas et al. (2000) and Latif and Grotzner (2000) identified a QB component in the Atlantic zonal mode, the latter clearly relating it to ENSO forcing, while Tseng and Mechoso (2001) did not find any external influence on the QB variability in equatorial Atlantic. Several studies also pointed out that the South Atlantic is dominated by shorter time scales as opposed to the North Atlantic (Zebiak 1993; Mo and Häkkinen 2001), which would be consistent with our finding the QB component confined to southern basin and the 5-yr one having links north of the equator. However, given the importance of decadal scales in the Atlantic variability the short QB scale has not been extensively documented so far.

## 4. The QB mode

### *a. Phase composites*

Although the model's QB component is relatively weak, visual examination of monthly sequences of SST anomaly maps (not shown) suggests its importance in anomaly phase reversals over the tropical Atlantic. To examine this component further, we now construct phase composites of ST and SLP, keyed to the SSA reconstructed time series. Prior to compositing, a Butterworth high-pass digital filter was applied at each ST and SLP grid point with cutoff frequency at 35 months to isolate sub-5-yr variability without filtering the fields too strongly in the QB range. All the subsequent results with regard to the QB component are obtained from this filtered data unless specified otherwise. Figure 8 illustrates the spatial ST and SLP structure of the QB

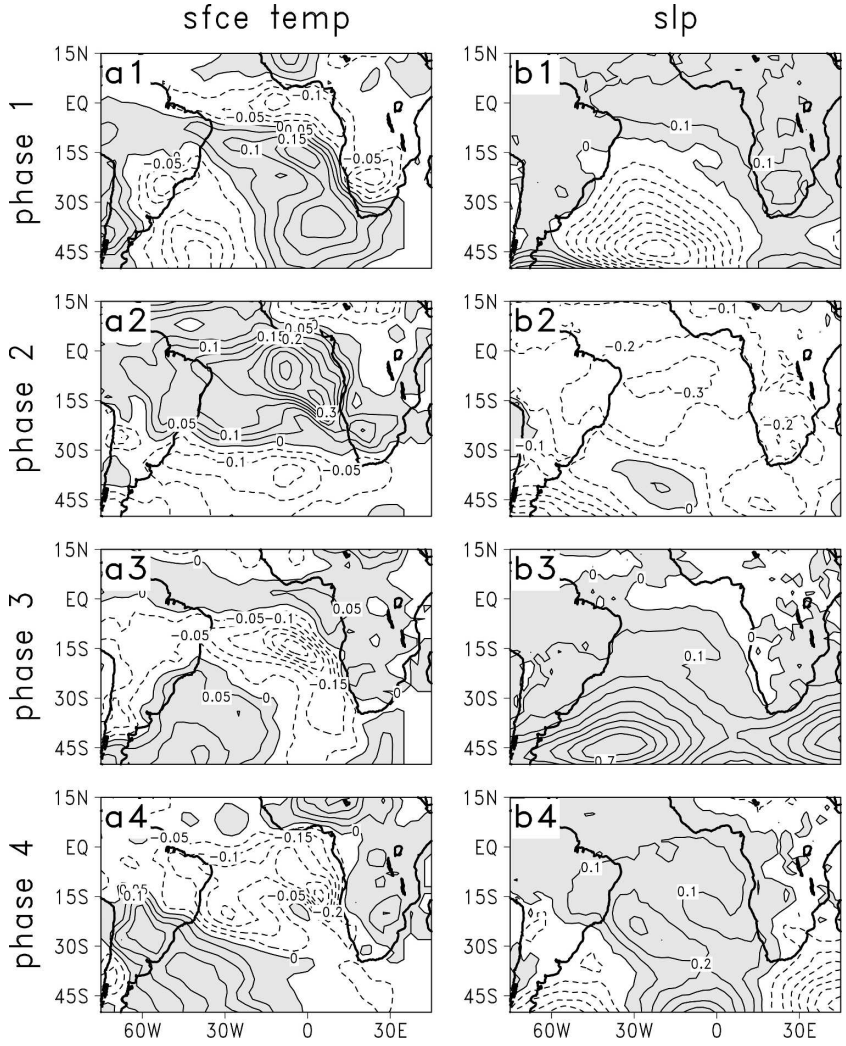


FIG. 8. Composite maps for the four phases of SSA-RPC56 (QB component) for (left) surface temperature (contours every 0.05 K; shading for positive anomalies) and (right) sea level pressure (contours every 0.1 hPa; shading for positive anomalies).

component through a cycle formed by compositing in phase intervals of ¼ period (i.e., about 6 months), using the technique of Plaut and Vautard (1994). Phases 2 and 4 correspond to the peak (or mature) phases of the quasi oscillation, and resemble the SVD1 pattern. Phases 1 and 3 correspond to the transition phases and are approximate mirror image of each other.

The picture that emerges is an apparent anticlockwise migration of ST anomalies. For example, negative ST anomalies over the southwestern Atlantic in phase 1 [Fig. 8(a1)] spread across the subtropics in phase 2 [Fig. 8(a2)]. They then migrate northward along the African coast in phase 3 [Fig. 8(a3)] and spread across the equatorial Atlantic during phase 4 [Fig. 8(a4)]. Thus, the mature negative phase 4 is preceded approximately 18 months before by negative anomalies over the southwestern Atlantic during phase 1. The latter (in stage 1) are associated with a negative subtropical SLP anomaly [Fig. 8(b1)], consistent with structure seen in SVD3 (Fig. 3). This evolution is consistent with the lagged relationship found between SVD1 and -3 and with the previous analysis of the observations by Robertson et al. (2003). The different stages of the migration are more evident with a higher partition of the cycle but a trade-off exists between the resolution and influence of sampling variability.

Similar propagation from the southeastern Atlantic to equatorial and western parts of the basin can also be found in the decomposition by Tourre et al. (1999) and in the results of Mo and Häkkinen (2001). Haarsma et al. (2003) pointed to downstream propagation of the anomalies, and Zhou and Carton (1998) found that the

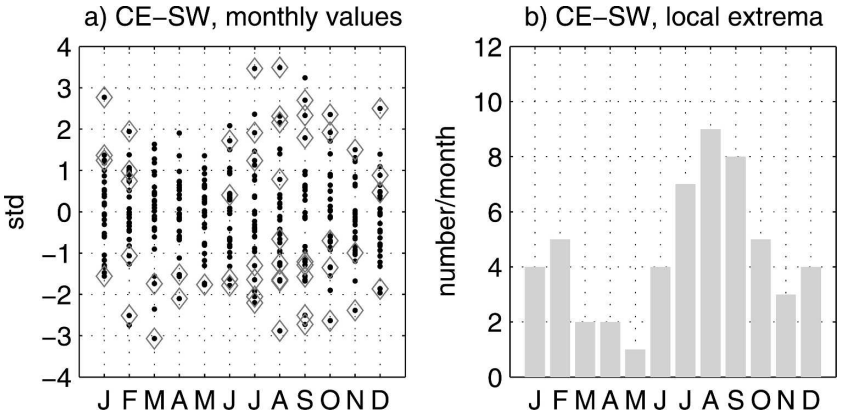


FIG. 9. "Dipolar" index CE-SW. (a) Monthly standardized values stratified by calendar month; dots—all values; diamonds—strongest events defined as CE and SW anomalies of opposite sign and the difference exceeding 0.7 standard deviation for at least 3 months; 3 months of strongest values are plotted. (b) Number of strongest events, stratified by calendar month.

wind–evaporation–SST (WES) feedback could generate SST anomaly propagation without ocean dynamics. The QB time scale could be set by the phase locking to the seasonal cycle itself, further investigated in the following paragraph.

### b. Seasonality

The phase locking of the QB mature-phase events to the seasonal cycle is shown in Fig. 9, in terms of difference between unfiltered SST over the tropical and southwestern Atlantic, using the grid boxes CE and SW in Fig. 10. When all the monthly values of this SST difference are plotted (Fig. 9a) there is a slight indication of lower variance in April–May and higher variance in July–September. However, more marked seasonality emerges when only strongest events are considered (i.e., index exceeding 0.7 standard deviation for at least 3 months, and CE and SW anomalies of opposite sign). The strongest dipolar events (Fig. 9a, diamonds) tend to occur in July–September with a minimum of occurrence in February–May, with the monthly counts shown in Fig. 9b. A phase locking to the seasonal cycle has been similarly found in the QB variability in the Indo–Pacific region by Barnett (1991) and Ropelewski et al. (1992) where the seasonality of air–sea coupling and the role of the heat content in the mixed layer had been highlighted (Brier 1978; Meehl 1987, 1993). In the Atlantic basin Frankignoul and Kestenare (2005) found that the tropical mode dominates in summer while Okumura et al. (2001) and Haarsma et al. (2003) pointed also to the seasonality of the extratropical atmospheric response in the Atlantic, consistent with our transition phases 1 and 3.

### c. Further evidence of quasi-biennial variability in model and reanalysis

As an independent measure of the counterclockwise migration of SST anomalies, Hovmoeller diagrams are plotted in Figs. 11 and 12 for both the model and observed data, high-pass filtered at 35 months. Three transects of SST are shown, along the arrows in Fig. 10 averaged over 15° of latitude or longitude respectively (shaded boxes), and for a 7-yr period where the signal is most regular.

The migration and consolidation of the anomalies

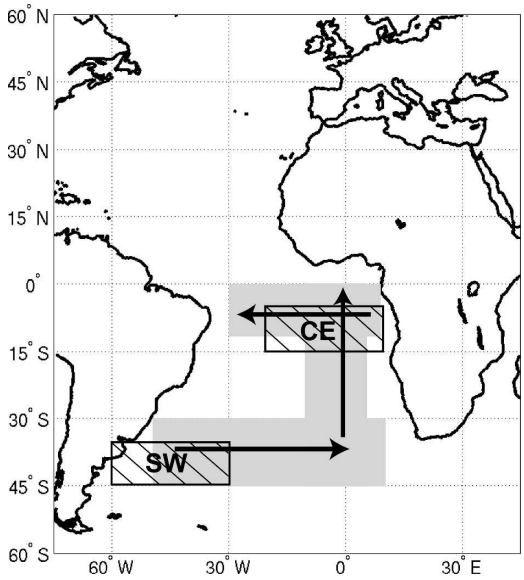


FIG. 10. Location of SST indices and bands used for Hovmoeller diagrams in Figs. 10–12.

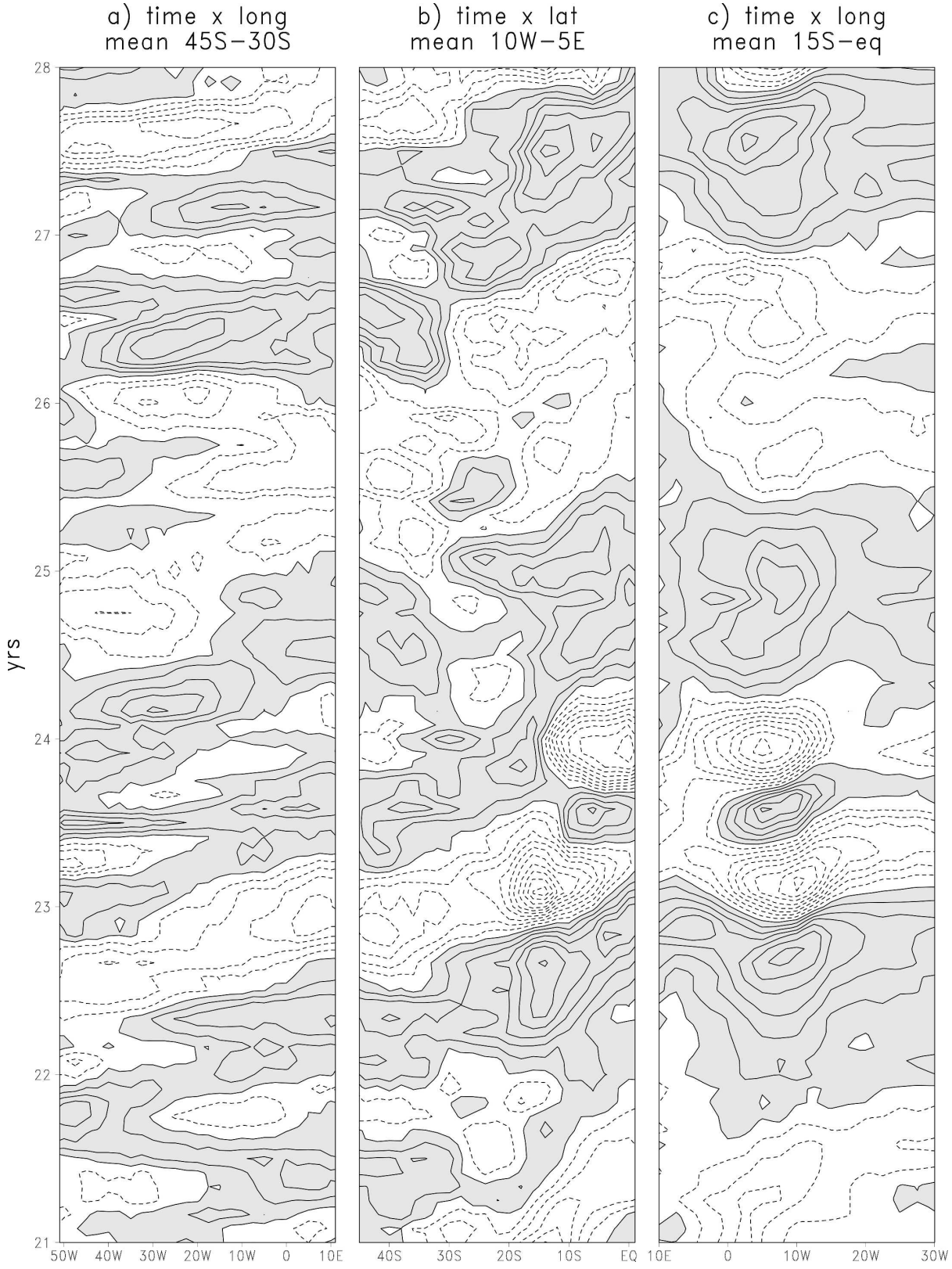


FIG. 11. Hoevmoller diagrams of high-pass-filtered surface temperatures along the three trajectories shown in Fig. 9 for UCLA-SOM years 21–28. Contours every 0.2 K; shadings for positive values.

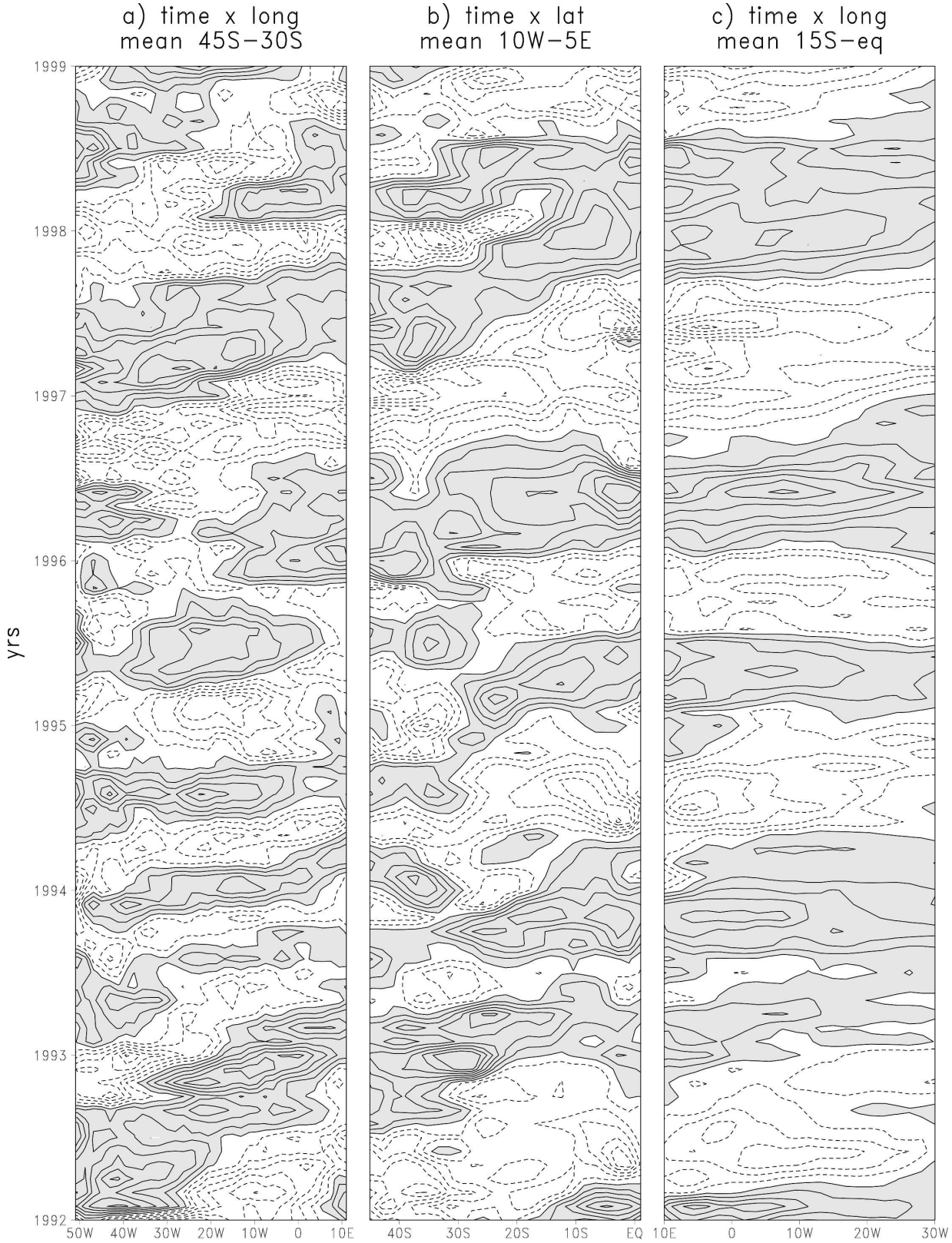


FIG. 12. Same as in Fig. 11, but for NCEP 1992–99.

from west to east in the subtropical South Atlantic is easy to follow in the first column of both figures. The migration is even more distinguishable in the northward trajectory along the coast of Africa in the middle plots and the anomalies strengthen as they move northward. The west–east spread in the subequatorial band seems quasi-instantaneous (right-hand side columns) but it can also be an artifact due to the average over 15° of latitude thus mixing of phases together. Note also that maxima of the anomalies tend to occur between 10°E and 10°W, to the south of West Africa, the anomalies being smaller farther west. The sequence of cool and warm SST anomalies in the tropical South Atlantic is slightly more regular in the reanalysis than in the model, suggesting that in the observations ocean dynamics could constructively interfere with surface-flux-induced anomalies. However, the variability in the extratropics has higher frequency than the modeled one, suggesting that in reality it is more independent from the tropical forcing than in the results of the model, following the lack of association of the southwestern region with the dominant SVD pattern in SLP. The ENSO influence via the PSA patterns (Mo 2000) may also account for the above feature.

### *d. Air–sea interactions in the QB mode*

To examine more closely what leads to the anomaly migration in the model, Figs. 13 and 14show phase composite maps of the QB cycle for downward net heat flux and its main components—the latent heat and shortwave radiation flux—together with low-level wind, horizontal moisture convergence, and midtropospheric vertical velocity. As expected the net heat flux anomalies exhibit structures directly related to subsequent phase of SST anomalies in Fig. 8, but their relation to the current SST anomalies is more subtle.

Phase 1 is mainly a reversed anomaly pattern to the one discussed by Venegas et al. (1997) and Sterl and Hazeleger (2003). In our case lower SLP overlies cold SST in the southwest of the basin [Fig. 8(b1)] and cyclonic circulation anomalies lead to reduced trade winds southeastward of north-eastern Brazil and enhanced westerlies between 40° and 30°S [Fig. 14(a1)]. Collocated with these circulation anomalies are upward heat flux anomalies, mainly latent flux [Figs. 13(a1) and 13(b1)] in the southwest and reduced evaporation, enhanced horizontal moisture convergence, and convection in the trade wind/SACZ region [Figs. 13(b1) and 14(a1)–(c1)] contributing to the respective cooling and warming of these regions. This is consistent with Venegas et al. (1997) local forcing of SST by the atmosphere and the Sterl and Hazeleger (2003) role of heat flux in generating SST anomalies. The shortwave radiative flux reaching the surface [Fig. 13(c1)] is weakly reduced in the SACZ region while it is enhanced in the southeastern subtropics, mainly due to the reduced stratus deck over warmer than usual ocean, which it contributes to warm further. This is consistent with a net heat gain (loss) by the ocean in the east and equator (southwest) found by Chaves and Nobre (2004) in the case of warm subtropical/cold extratropical South Atlantic. The major difference with their results concerns the presence of tropical SST anomalies in our case that initiate a strong atmospheric response in the SACZ and ITCZ regions, consistent with SST forcing of Robertson et al. (2003). This further warms the tropical ocean by increasing moisture convergence and reducing the evaporation.

In phase 2 warm tropical and subtropical waters force widespread low SLP [Figs. 8(a2) and 8(b2)] and upward motion anomalies [Fig. 14(c2)], mostly in ITCZ and western part of the basin. Shortwave radiation into the surface is reduced [Fig. 13(c2)] following a denser cloud cover while reduced evaporation only concerns a narrow band in the ITCZ region [Fig. 13(b2)]. This band is collocated with maximum convection and horizontal moisture convergence anomalies [Figs. 14(c2) and 14(b2)], at the expense of regions immediately poleward that loose heat by enhanced evaporation, roughly linked with divergent moisture anomalies. The reduced evaporation in the ITCZ region, together with enhanced shortwave radiation in the eastern tropical South Atlantic [Figs. 13(b2) and 13(c2)], helps the persistence of warm anomalies at the equator while the subtropics cool down. Despite reduced evaporation, strong shortwave deficit in the western tropical Atlantic leads to progressive SST cooling in this region as suggested by Chaves and Nobre (2004). The southwestern part of the basin undergoes progressive warming [Fig. 13(a2)], partly linked to weak anomalies in the low-level horizontal moisture convergence and wind [Figs. 14(b2) and 14(a2)]. The latter are related to the tropical forcing: enhanced convection in the equatorial regions generates anticyclonic circulation in the upper levels along with a Rossby wave train with a cyclonic center southwest of Africa (not shown). This translates at the surface into the weak cyclonic circulation in the southeastern Atlantic [Fig. 14(a2)], while anticyclonic circulation builds up in the southwestern part, under the influence of the poleward extension of upper-level anticyclonic anomalies that have an equivalent-barotropic vertical structure in the extratropics.

In phase 3 most of the subtropical Atlantic has cooled except the ITCZ region where reduced evaporation linked to horizontal moisture convergence kept warming the SST. This phase resembles the patterns

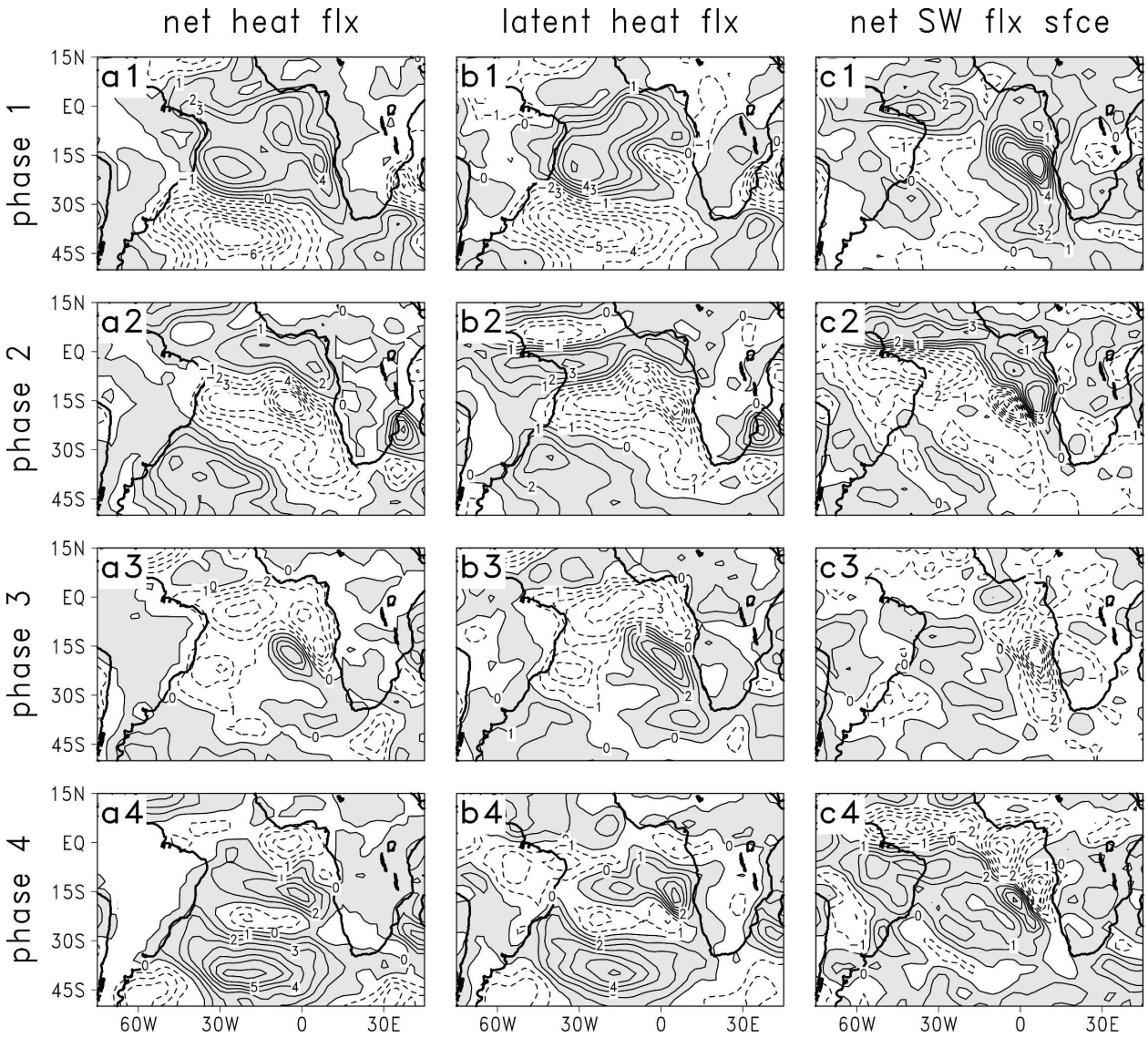


FIG. 13. Composite maps for the four phases of SSA-RPC56 (QB component) for (left) net heat, (middle) latent heat, and (right) shortwave radiative fluxes at the surface (contours every 10 W $m^{-2}$, shading for positive values, into the surface).

discussed by Venegas et al. (1997) and Sterl and Hazeleger (2003). High SLP overlies warmer SST in the southwest [Fig. 8(b3)], while trade winds have strengthened [Fig. 14(a3)]. In agreement with cooler SST, the convection and moisture convergence are reduced in the SACZ region [Fig. 14(c3)], also seen in increased downward shortwave radiation [Fig. 13(c3)]. The cooling of the surface further spreads westward and equatorward due to WES feedback: increased evaporation [Fig. 13(b3)] and reduced moisture convergence [Fig. 14(b3)] due to increased trades off northeastern Brazil and transequatorial wind anomalies [Fig. 14(a3)]. As pointed previously, positive SST–shortwave feedback operates in the east over cold anomalies [Fig. 13(c3)], partly offsetting surface warming related to reduced evaporation (Fig. 13b3).

In phase 4 substantial warming of the subtropics, and southern and eastern extratropics, occurs [Fig. 13(a4)]. In the southern extratropics this is mainly linked with reduced evaporation [Fig. 13(b4)] collocated with a higher pressure center [Fig. 8(b4)] and anticyclonic circulation with reduced westerlies [Fig. 14(a4)]. This center is the surface manifestation of the upper-level high pressure center (with an equivalent-barotropic vertical structure), related to the Rossby wave generated by changes in the tropical convection. As in phase 2, a reversed pressure anomaly occurs westward of this center, with lower pressure at the surface [Fig. 8(b4)], low-

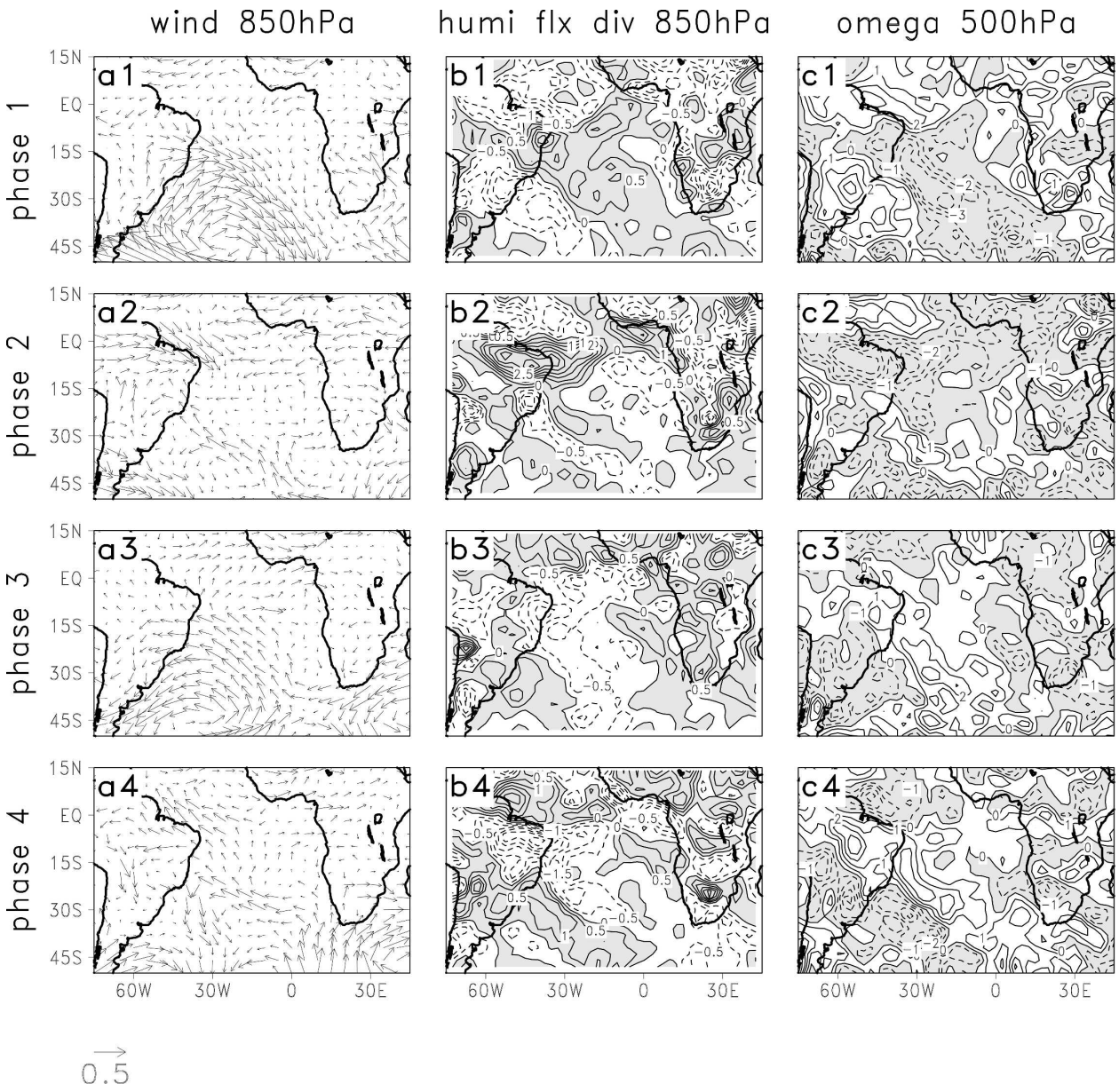


FIG. 14. Composite maps for the four phases of SSA-RPC56 (QB component) for (left) wind at 850 hPa (in m $s^{-1}$; scale at the bottom), (middle) specific humidity flux horizontal divergence at 850 hPa (contour every 0.5 $10^{-6}$ gm (kg s)$^{-1}$, convergence—positive values—shaded), and (right) vertical velocity at 500 hPa (contour every $10^{-3}$ Pa $s^{-1}$, upward anomalies—negative values—shaded).

level cyclonic circulation [Fig. 14(a4)], and enhanced evaporation [Fig. 13(b4)], leading to negative anomalies in the southwestern South Atlantic in phase 1. Reduced evaporation and enhanced shortwave radiation are responsible for the warming of the central subtropics [Figs. 13(b4) and 13(c4)], while in the western subtropics warming occurs mainly through enhanced shortwave flux, offsetting enhanced evaporation linked to higher pressures [Fig. 8(b4)], reduced convection, and moisture convergence south of equator [Figs. 14(b4) and 14(c4)]. In the equatorial regions the cooling tendency persists due to negative shortwave feedback in the enhanced convection regions in the west and positive feedback over cooler waters of Gulf of Guinea.

### *e. Hypothesized mechanism*

Most of the studies of the variability in the tropical Atlantic have focused on ocean dynamics as the main process generating SST anomalies with heat fluxes mainly damping the anomalies. For example, Franki-

gnoul and Kestenare (2002) found an overall negative heat flux feedback in the tropical Atlantic, mainly due to the latent heat flux, with only a small contribution from radiative component. However, in our model study the evaporation does not always act as a negative feedback. Thermodynamic air–sea interactions generate well-defined SST variability in the model with propagating characteristics in the following sequence.

During a well-developed tropical zonal SST anomaly in the boreal summer the tropical atmosphere in the deep convective region mainly responds to SST anomalies with evaporation feedback being positive and the negative feedback provided by the radiation. Anomalies in convection generate a Rossby wave train into extratropics where they force reversed SST anomalies via changes in evaporation due to anomalous atmospheric circulation at the surface. While tropical SST anomalies slowly decay in the following winter, reversed SST anomalies are generated in the southeastern Atlantic—a region dominated by shallow clouds. Here the radiative feedback helps building the anomalies while the evaporative feedback damps them. Subtropical anomalies induce perturbations in the seasonal cycle of the main convective zones: the northward shift of the ITCZ and development of the West African monsoon and decay of the SACZ from boreal spring to summer. This in turn generates SST anomalies in the Tropics and further affects the tropical convection in boreal summer.

Crucial to this sequence are differences in the feedback between SST and the major components of the net heat flux (the latent heat flux and the net shortwave radiative flux) between the eastern and western parts of the basin. In the western tropical and South Atlantic, dominated by deep convection in the SACZ and ITCZ regions, the SST–evaporation feedback is found to be positive, mainly due to low-level moisture convergence from adjacent regions, while the SST–shortwave flux feedback is negative because of the effects of the deep convective clouds, sheltering the surface. In the eastern tropical and South Atlantic, dominated by shallow clouds, SST–shortwave radiation feedback is positive and tends to increase the persistence of SST anomalies while the evaporation tends to damp it.

Such differences between feedback in the eastern and western parts of the basin have been pointed out by previous studies in the Pacific (Xie 1996; Kitoh et al. 1999). Positive SST–evaporation feedback in the convective regions in the western tropical Atlantic has previously been found by Chang et al. (2000) while Okumura et al. (2001) and Chaves and Nobre (2004) highlighted the positive SST–low-level clouds feedback in the subtropical Atlantic. A closer examination of Frankignoul and Kestenare's (2002) figures reveals a weak but consistent positive radiative feedback in southeastern tropical Atlantic in all seasons and a negative radiative feedback in the ITCZ.

While the exact shape of the anomaly structures differs from the results of Frankignoul and Kestenare (2005), we found damping effects of latent heat flux on SST in the southeastern Atlantic and that of radiative heat flux in the deep convective region to the west of main SST anomalies. Our results are thus consistent with their analyses. The major difference resides in a stronger role of radiative feedback, which could be model dependant. Given the persistence of the anomalies (*e*-folding time of 6 months) and the presence of long-time-scale variability in their study, ±2 month lagged correlations or composites may not show substantial changes in the heat flux patterns.

The temporal and spatial scales of the SST anomalies are set by the existence of deep convection and the possibility of advection of external moisture. We suggest that the time and space scales of the QB variability are strongly related to the seasonal cycle and to the existence and location of deep and shallow cloud regions and interactions between Tropics and extratropics. In boreal summer early fall, the tropical atmosphere mainly responds to the underlying anomaly maintained by the positive SST–evaporation feedback in the convective region, baroclinic in nature and similar to the one obtained in forced simulations by Robertson et al. (2003) and Okumura et al. (2001). As in the latter study, this response further forces an equivalent-barotropic atmospheric response in the subtropics and extratropics, forcing the SST, and consistent with analyses by Venegas et al. (1997) and Sterl and Hazeleger (2003). This provides the link from the Tropics to extratropics.

Tropical SST change in response to changes in evaporation and shortwave radiation, linked to variations in low-level winds and subtropical high pressure center. This provides the link between the extra- and subtropics and the Tropics, and is consistent with the SST evolution found in observations by Robertson et al. (2003). It also indicates that the sub- and extratropical South Atlantic may contain useful information on the evolution of tropical SST. However, most of the analyses and prediction systems have focused to date on variability north of 30°S and links with eastern tropical Pacific (e.g., Tourre et al. 1999; Repelli and Nobre 2004).

## 5. Summary and discussion

We have shown that the main characteristics of coupled variability in the South Atlantic region gener-

ated by an AGCM coupled to a SOM in the Atlantic with no external forcing are very similar to the ones previously documented in the observations. They consist of the following:

1) A predominantly tropical mode akin to the equatorial zonal mode (Zebiak 1993) with a large-scale Matsuno–Gill-type baroclinic response in the tropical atmosphere, similar to the atmospheric behavior in simulations forced with similar SST structures (Robertson et al. 2003). This mode has been generated here only by air–sea thermodynamic interactions in the Atlantic with no external influences. An atmospheric bridge to the South Atlantic in the form of a Rossby wave further forces an extratropical oceanic response leading to a dipolar structure of SST anomalies.
2) A subtropical mode, consistent with the descriptions of Venegas et al. (1997) and Sterl and Hazeleger (2003), linked to atmospheric forcing of the ocean via variations in the strength of subtropical high and southeasterlies. It exhibits an equivalent-barotropic structure and is associated with an extratropical wave train that arises from internal atmospheric variability in the model, but could also be externally forced in the observations by PSA-type adjustment to ENSO (Cook 2001; Mo 2000). Haarsma et al. (2005) have previously found that air–sea thermodynamic interaction is crucial for this mode while the positive feedback in the equatorward part of the structure enables its development and persistence.

Both simulated modes have seasonality consistent with the observations: the subtropical mode, more boreal winter to spring precedes the tropical one, which peaks in boreal summer to fall (cf. Venegas et al. 1996; Houghton and Tourre 1992; Zebiak 1993; Carton and Huang 1994; Ruiz-Barradas et al. 2000; Robertson et al. 2003).

Our decomposition differs from previous studies of observed ocean–atmosphere interactions over the South Atlantic (e.g., Venegas et al. 1997; Sterl and Hazeleger 2003), by the use of the correlation matrix, which excludes the influence of the anomaly amplitude on the results and thus tends to emphasize the tropical variability in the South Atlantic variability. The tropical mode, however, accounts for twice the squared correlation fraction in our model as compared to the reanalysis, highlighting the role of other types of variability in the region, notably the ENSO forcing, absent from the simulations. The mechanism leading to this mode may also be overestimated in the model due to an oversensitivity of the cloud–SST feedback in the stratus region and absence of ocean dynamics. The tropical–extratropical atmospheric bridge seems also less robust in the reanalysis data where the PSA-type teleconnections are generated during ENSO and can extend into the South Atlantic (Mo 2000). Nonetheless, the links and mechanisms isolated in this study could be important during ENSO-neutral conditions as well as in the South Atlantic response to ENSO forcing.

Despite the above caveats and the limited length of the simulation we have found the dominant time scales of the simulated tropical mode to be very similar to the observed ones, in both cases exhibiting a red power spectrum and identifiable oscillatory components with periods near 2 and 5 yr. Previous observational studies have identified a modest QB component in the equatorial Atlantic (Ruiz-Barradas et al. 2000; Dommenget and Latif 2000; Latif and Grotzner 2000; Tseng and Mechoso 2001) or more broadly in the tropical Atlantic (Servain 1991; Tourre et al. 1999; Mo and Häkkinen 2001), and longer interannual time scales have been associated with northern Atlantic (Servain 1991; Tourre et al. 1999; Rajagopalan et al. 1998; Mo and Häkkinen 2001). In agreement with the above studies we found that the QB component is largely confined to the southern and equatorial Atlantic while the 5 yr component is associated with cross-equatorial interactions: the WES feedback across the equator postulated by Chang et al. (1997) may increase the interannual persistence of the cross-equatorial SST anomaly gradient that may arise occasionally between the tropical parts of southern and northern Atlantic modes of variability. This view is consistent with the results of Houghton and Tourre (1992), Enfield et al. (1999), Dommenget and Latif (2000), Sutton et al. (2000), and Haarsma et al. (2003). Investigation of this aspect was however beyond the scope of this paper.

The QB component in the Atlantic had been previously linked to the QB component of ENSO (Mo and Häkkinen 2001) or to equatorial ocean dynamics (Tseng and Mechoso 2001) while it arises purely from thermodynamic air–sea interactions in our case. It appears to be associated with an anticlockwise migration of SST anomalies around the South Atlantic basin, phase locked to the seasonal cycle. This most clearly involves the subtropical mode preceding the tropical mode, with the transition taking place from austral summer–fall, to boreal summer, also seen in observed SSTs (Robertson et al. 2003). Some indication of migration from the subtropics to the Tropics along the African coast can be seen in Tourre et al.'s (1999) 2.7-yr mode and from central subtropical South Atlantic into tropical South Atlantic in their 3.5-yr mode. Using an AGCM-SOM, Barreiro et al. (2004) have concluded that the austral summer atmospheric variability (and to

a lesser extent the winter variability) can play a preconditioning role in the onset of the interhemispheric anomalies in the deep Tropics during the following austral fall. The main difference with our results is that Barreiro et al.'s results have emphasized the preconditioning of the meridional mode of Tropical Atlantic Variability (TAV) during March–May, while our study identifies preconditioning of the zonal mode of TAV during boreal summer. No temporal scale separation was performed in their analysis and their composite may include some longer-time-scale persistence of the tropical anomalies associated with the cross-equatorial SST gradient as discussed above. The results of this study show strong similarities with the sequence of anomalies and the timing described by Mo and Häkkinen (2001): the initial June–August (JJA) anomaly along the African coast strengthens and migrates westward, while an opposite sign anomaly builds in the southwestern Atlantic in September–November (SON); in December–February (DJF) anomalies along the African coast vanish and the initial anomaly is confined to the western tropical Atlantic; finally, opposite sign anomalies appear in the southeastern Atlantic, along the African coast in March–May (MAM) while the initial anomaly totally disappeared. However, these authors associate this sequence with SST anomalies in the eastern Pacific while in our case similar behavior arises from thermodynamic interactions within the basin. Crucial to this propagation and its time scales is the existence and seasonality of the deep convective regions in the Tropics/western subtropics and shallow cloud regions in southeastern South Atlantic with positive/negative feedbacks between SST and latent/radiative heat flux in the former region and reversed feedback in the latter.

Variability in the equatorial Atlantic has long been associated with equatorial dynamics (Zebiak 1993; Servain and Dessier 1999), and Frankignoul and Kestenare (2005) mainly concluded on damping effects of the heat flux outside the western equatorial Atlantic. However, SST variability is no longer related to the thermocline depth poleward of about 7.5°S/N (Carton et al. 1996), and on the other hand, latent heat flux seems to modulate SST variability generated by the equatorial dynamics (Zhou and Carton 1998). Dommenget and Latif (2000) further found no major difference in the main modes of variability in the tropical Atlantic simulated by a fully coupled GCM or AGCM coupled to a mixed-layer model. Moreover, the interference between thermodynamic and dynamic coupling in the equatorial region seems to be constructive: warm equatorial SST anomalies near the equator are associated with relaxed winds in our case, which may depress the thermocline, leading to further warming of the equatorial Atlantic. Latent heat flux anomalies were found to play an important role in the dynamics of the subtropical dipole, offsetting oceanic processes in the study of Haarsma et al. (2003), and Chaves and Nobre (2004) found the SST–cloud feedback in the subtropics more important than oceanic processes. By analyzing the mechanisms by which thermodynamic-only air–sea interactions give rise to SST variability similar to the observed one we do not exclude the dominant role of ocean dynamics, particularly in the equatorial Atlantic, nor the tropical–extratropical link such as those proposed by Florenchie et al. (2004). Rather we tried to elucidate the reasons of the simulated variability. The lack of ocean dynamics in our simulation can partly account for differences in shape and location of the patterns isolated here as compared to the observation.

The suggested anticlockwise progression of anomalies and mechanism with the distinction between feedbacks in west and east and tropical–extratropical interactions could affect the impacts of external forcings such as PSA in the extratropics and/or zonal circulation in the Tropics related to ENSO. Underestimation of positive heat flux feedbacks may lead to a too-strong damping of SST in coupled models, and thus to lack of SST persistence as pointed out by Frankignoul et al. (2004). Systematic inclusion and analyses of both the SST–evaporation and SST–shortwave feedbacks in the Atlantic ocean and, as much as possible, extension of analyses and simulations to the southern extratropics could provide important elements for the seasonal prediction of SST in the equatorial and South Atlantic. So far, however, most of the statistical or dynamical seasonal forecast systems have used mostly tropical information (cf. Penland and Matrosova 1998; Repelli and Nobre 2004; Barreiro et al. 2005).

*Acknowledgments.* This paper is funded in part by a grant/cooperative agreement from the National Oceanic and Atmospheric Administration, NA05OAR4311004, NA03OAR4320179, and NA06GP0511. The NCEP–NCAR reanalysis data were provided through the NOAA/Climate Diagnostics Center (http://www.cdc.noaa.gov). The views expressed herein are those of the author(s) and do not necessarily reflect the views of NOAA or any of its subagencies.

## REFERENCES

Allen, M. R., and L. A. Smith, 1996: Monte Carlo SSA: Detecting irregular oscillations in the presence of colored noise. *J. Climate,* **9,** 3373–3404.

Barnett, T. P., 1991: The interaction of multiple time scales in the tropical climate system. *J. Climate,* **4,** 269–285.

Barreiro, M., A. Giannini, P. Chang, and R. Saravannan, 2004: On the role of the South Atlantic atmospheric circulation in tropical Atlantic variability. *Earth's Climate: The Ocean-Atmosphere Interaction, Geophys. Monogr.,* Vol. 147, Amer. Geophys. Union, 143–156.

——, P. Chang, R. Saravannan, and A. Giannini, 2005: Dynamical elements of predicting boreal spring tropical Atlantic sea-surface temperatures. *Dyn. Atmos. Oceans,* **39,** 61–85.

Bretherton, C. S., C. Smith, and J. M. Wallace, 1992: An intercomparison of methods for finding coupled patterns in climate data. *J. Climatol.,* **5,** 541–560.

Brier, G. W., 1978: The quasi-biennial oscillation and feedback processes in the atmosphere–ocean–earth system. *Mon. Wea. Rev.,* **106,** 938–946.

Carton, J. A., and B. Huang, 1994: Warm events in the tropical Atlantic. *J. Phys. Oceanogr.,* **24,** 888–903.

——, X. Cao, B. S. Giese, and A. M. da Silva, 1996: Decadal and interannual SST variability in the tropical Atlantic Ocean. *J. Phys. Oceanogr.,* **26,** 1165–1175.

Chang, P., L. Ji, and H. Li, 1997: A decadal climate variation in the tropical Atlantic Ocean from thermodynamic air-sea interactions. *Nature,* **385,** 516–518.

——, R. Saravanan, L. Ji, and G. C. Hegerl, 2000: The effect of local sea surface temperatures on atmospheric circulation over the tropical Atlantic sector. *J. Climate,* **13,** 2195–2216.

Chaves, R. R., and P. Nobre, 2004: Interactions between sea surface temperature over the South Atlantic Ocean and the South Atlantic convergence zone. *Geophys. Res. Lett.,* **31,** L03204, doi:10.1029/2003GL018647.

Cook, K. H., 2001: A Southern Hemisphere wave response to ENSO with implications for southern Africa precipitation. *J. Atmos. Sci.,* **58,** 2146–2162.

Delecluse, P., J. Servain, C. Levy, K. Arpe, and L. Bengtsson, 1994: On the connection between the 1984 Atlantic warm event and the 1982–83 ENSO. *Tellus,* **46A,** 448–464.

Dommenget, D., and M. Latif, 2000: Interannual to decadal variability in the tropical Atlantic. *J. Climate,* **13,** 777–792.

Enfield, D. B., and D. A. Mayer, 1997: Tropical Atlantic sea surface temperature variability and its relation to El Nino-Southern Oscillation. *J. Geophys. Res.,* **102,** 929–946.

——, A. M. Mestas-Nuez, D. A. Mayer, and L. Cid-Serrano, 1999: How ubiquitous is the dipole relationship in tropical Atlantic sea surface temperatures? *J. Geophys. Res.,* **104,** 7841–7848.

Florenchie, P., C. J. C. Reason, J. R. E. Lutjeharms, M. Rouault, C. Roy, and S. Masson, 2004: Evolution of interannual warm and cold events in the southeast Atlantic Ocean. *J. Climate,* **17,** 2318–2334.

Frankignoul, C., and E. Kestenare, 2002: The surface heat flux feedback. Part I: Estimates from observations in the Atlantic and the North Pacific. *Climate Dyn.,* **19,** 633–647.

——, and ——, 2005: Air–sea interactions in the tropical Atlantic: A view based on lagged rotated maximum covariance analysis. *J. Climate,* **18,** 3874–3890.

——, ——, M. Botzet, A. F. Carril, H. Drange, A. Pardaens, L. Terray, and R. Sutton, 2004: An intercomparison between the surface heat flux feedback in five coupled models, COADS and the NCEP reanalysis. *Climate Dyn.,* **22,** 373–388.

Ghil, M., and Coauthors, 2002: Advanced spectral methods for climatic time series. *Rev. Geophys.,* **40,** 1003, doi:10.1029/2000RG000092.

Giannini, A., R. Saravanan, and P. Chang, 2004: The preconditioning role of tropical Atlantic variability in the development of the ENSO teleconnection: Implications for the prediction of Nordeste rainfall. *Climate Dyn.,* **22,** 839–855.

Gill, A. E., 1980: Some simple solutions for heat-induced tropical circulation. *Quart. J. Roy. Meteor. Soc.,* **106,** 447–462.

Goddard, L., and S. J. Mason, 2002: Sensitivity of seasonal climate forecasts to persisted SST anomalies. *Climate Dyn.,* **19,** 619–631.

Haarsma, R. J., E. J. D. Campos, and F. Molteni, 2003: Atmospheric response to South Atlantic SST dipole. *Geophys. Res. Lett.,* **30,** 1864, doi:10.1029/2003GL017829.

——, ——, W. Hazeleger, C. Severijns, A. R. Piola, and F. Molteni, 2005: Dominant modes of variability in the South Atlantic: A study with a hierarchy of ocean–atmosphere models. *J. Climate,* **18,** 1719–1735.

Houghton, R. W., and Y. M. Tourre, 1992: Characteristics of low-frequency sea surface temperature fluctuations in the tropical Atlantic. *J. Climate,* **5,** 765–772.

Huang, H.-P., A. W. Robertson, and Y. Kushmir, 2005: Atlantic SST gradient and the influence of ENSO. *Geophys. Res. Lett.,* **32,** L20706, doi:10.1029/2005GL023944.

Kalnay, E., and Coauthors, 1996: The NCEP/NCAR 40-Year Reanalysis Project. *Bull. Amer. Meteor. Soc.,* **77,** 437–471.

Kitoh, A., T. Motoi, and H. Koide, 1999: SST variability and its mechanism in a coupled atmosphere–mixed layer ocean model. *J. Climate,* **12,** 1221–1239.

Köhler, M., 1999: Explicit prediction of ice clouds in general circulation models. Ph.D. dissertation, University of California, Los Angeles, 167 pp.

Latif, M., and A. Grotzner, 2000: The equatorial Atlantic oscillation and its response to ENSO. *Climate Dyn.,* **16,** 213–218.

Li, J.-L. F., M. Köhler, J. D. Farrara, and C. R. Mechoso, 2002: The impact of stratocumulus cloud radiative properties on surface heat fluxes simulated with a general circulation model. *Mon. Wea. Rev.,* **130,** 1433–1441.

Mann, M. E., and J. Park, 1993: Spatial correlations of interdecadal variation in global surface temperatures. *Geophys. Res. Lett.,* **20,** 1055–1058.

——, and J. M. Lees, 1996: Robust estimation of background noise and signal detection in climatic time series. *Climatic Change,* **33,** 409–445.

Meehl, G. A., 1987: The annual cycle and interannual variability in the tropical Pacific and Indian Ocean regions. *Mon. Wea. Rev.,* **115,** 27–50.

——, 1993: A coupled air–sea biennial mechanism in the tropical Indian and Pacific regions: Role of the ocean. *J. Climate,* **6,** 31–41.

Mehta, V. M., 1998: Variability of the tropical ocean surface temperatures at decadal–multidecadal timescales. Part I: The Atlantic Ocean. *J. Climate,* **11,** 2351–2375.

——, and T. Delworth, 1995: Decadal variability of the tropical Atlantic Ocean surface temperature in shipboard measurements and in a global ocean–atmosphere model. *J. Climate,* **8,** 172–190.

Mo, K. C., 2000: Relationships between low-frequency variability in the Southern Hemisphere and sea surface temperature anomalies. *J. Climate,* **13,** 3599–3610.

——, and S. Häkkinen, 2001: Interannual variability in the tropical Atlantic and linkages to the Pacific. *J. Climate,* **14,** 2740–2762.

Murtugudde, R. G., J. Ballabrera-Poy, J. Beachamp, and A. J. Busalacchi, 2001: Relationship between zonal and meridional modes in the tropical Atlantic. *Geophys. Res. Lett.,* **28,** 4463–4466.

Okumura, Y., S.-P. Xie, A. Numaguti, and Y. Tanimoto, 2001: Tropical Atlantic air-sea interaction and its influence on the NAO. *Geophys. Res. Lett.,* **28,** 1507–1510.

Pan, D.-M., and D. A. Randall, 1998: A cumulus parameterization with a prognostic closure. *Quart. J. Roy. Meteor. Soc.,* **124,** 949–981.

Penland, C., and L. Matrosova, 1998: Prediction of tropical Atlantic sea surface temperatures using linear inverse modeling. *J. Climate,* **11,** 483–495.

Philander, S. G. H., D. Gu, G. Lambert, T. Li, D. Halpern, N.-C. Lau, and R. C. Pacanowski, 1996: Why the ITCZ is mostly north of the equator. *J. Climate,* **9,** 2958–2972.

Plaut, G., and R. Vautard, 1994: Spells of low-frequency oscillations and weather regimes in the Northern Hemisphere. *J. Atmos. Sci.,* **51,** 210–236.

Rajagopalan, B., Y. Kushnir, and Y. M. Tourre, 1998: Observed decadal midlatitude and tropical Atlantic climate variability. *Geophys. Res. Lett.,* **25,** 3967–3970.

Rayner, N. A., E. B. Horton, D. E. Parker, C. K. Folland, and R. B. Hackett, 1996: Version 2.2 of the global sea-ice and sea surface temperature data set, 1903–1994. Climate Research Tech. Note 74, 43 pp.

Repelli, C., and P. Nobre, 2004: Statistical prediction of sea-surface temperature over the tropical Atlantic. *Int. J. Climatol.,* **24,** 45–55.

Reynolds, R. W., and T. M. Smith, 1994: Improved global sea surface temperature analyses using optimum interpolation. *J. Climate,* **7,** 929–948.

Robertson, A. W., C. R. Mechoso, and Y.-J. Kim, 2000: The influence of Atlantic sea surface temperature anomalies on the North Atlantic Oscillation. *J. Climate,* **13,** 122–138.

——, J. D. Farrara, and C. R. Mechoso, 2003: Simulations of the atmospheric response to South Atlantic sea surface temperature anomalies. *J. Climate,* **16,** 2540–2551.

Ropelewski, C. F., M. S. Halpert, and X. Wang, 1992: Observed tropospheric biennial variability and its relationship to the Southern Oscillation. *J. Climate,* **5,** 594–614.

Ruiz-Barradas, A., J. A. Carton, and S. Nigam, 2000: Structure of interannual-to-decadal climate variability in the tropical Atlantic sector. *J. Climate,* **13,** 3285–3297.

Saravanan, R., and P. Chang, 2004: Thermodynamic coupling and predictability of tropical sea surface temperature. *Earth's Climate: The Ocean-Atmosphere Interaction, Geophys. Monogr.,* Vol. 147, Amer. Geophys. Union, 171–180.

Servain, J., 1991: Simple climatic indices for the tropical Atlantic Ocean and some applications. *J. Geophys. Res.,* **96,** 15 137–15 146.

——, and A. Dessier, 1999: Relationship between equatorial and meridional modes of climatic variability in the tropical Atlantic. *Geophys. Res. Lett.,* **26,** 485–488.

Sterl, A., and W. Hazeleger, 2003: Coupled variability and air-sea interaction in the South Atlantic Ocean. *Climate Dyn.,* **21,** 559–571.

Sutton, R. T., S. P. Jewson, and D. P. Rowell, 2000: The elements of climate variability in the tropical Atlantic. *J. Climate,* **13,** 3261–3284.

Tourre, Y. M., B. Rajagopalan, and Y. Kushnir, 1999: Dominant patterns of climate variability in the Atlantic Ocean during the last 136 years. *J. Climate,* **12,** 2285–2299.

Tseng, L., and C. R. Mechoso, 2001: A quasi-biennial oscillation in the equatorial Atlantic Ocean. *Geophys. Res. Lett.,* **28,** 187–190.

Vautard, R., P. Yiou, and M. Ghil, 1992: Singular Spectrum Analysis: A toolkit for short, noisy, chaotic time series. *Physica D,* **58,** 95–126.

Venegas, S. A., L. A. Mysak, and D. N. Straub, 1996: Evidence for interannual and interdecadal climate variability in the South Atlantic. *Geophys. Res. Lett.,* **23,** 2673–2676.

——, ——, and ——, 1997: Atmosphere–ocean coupled variability in the South Atlantic. *J. Climate,* **10,** 2904–2920.

Xie, S.-P., 1996: Westward propagation of latitudinal asymmetry in a coupled ocean–atmosphere model. *J. Atmos. Sci.,* **53,** 3236–3250.

Yu, J.-Y., and C. R. Mechoso, 2001: An Indo-Pacific SST teleconnection pattern during ENSO. *Proc. 12th Symp. on Global Change and Climate Variations,* Albuquerque, NM, Amer. Meteor. Soc., 293–296.

Zebiak, S. E., 1993: Air–sea interaction in equatorial Atlantic region. *J. Climate,* **6,** 1567–1586.

Zhou, Z., and J. A. Carton, 1998: Latent heat flux and interannual variability of the coupled atmosphere–ocean system. *J. Atmos. Sci.,* **55,** 494–501.